Am J Transl Res 2023;15(2):896-913
www.ajtr.org /ISSN:1943-8141/AJTR0146186

Original Article

ETS-1/c-Met drives resistance to sorafenib in hepatocellular carcinoma

Yongfang Ma[1,2*], Xueke Liu[2*], Xiaolong Tang[1]

[1]Medical School, Anhui University of Science and Technology, Huainan 232001, Anhui, China; [2]Department of Clinical Laboratory Medicine, The Fourth Affiliated Hospital, Zhejiang University School of Medicine, Yiwu 322000, Zhejiang, China. [*]Equal contributors.

Received August 28, 2022; Accepted December 27, 2022; Epub February 15, 2023; Published February 28, 2023

Abstract: Background: The purpose of this study was to clarify the molecular regulatory mechanism of c-Met upregulated expression and elucidate the molecular mechanisms by which c-Met overexpression and activation drive progression and sorafenib resistance in hepatocellular carcinoma (HCC). Methods: The resistance index was calculated. Bioinformatic techniques were applied to predict the transcription factors that bind and their binding sites on the c-Met promoter. Chromatin immunoprecipitation assays were implemented to verify the prediction results. To determine the regulatory mechanisms and effects of c-Met on sorafenib resistance in HCC, c-Met expression and activation were down-regulated by siRNA and inhibitor in in vivo and vitro experiments, while a parental cell line (Huh-7) was transfected with the adenovirus that upregulated c-Met expression. Results: c-Met expression was increased in HCC sorafenib-resistant cells. Functional findings suggested that c-Met overexpression and activation drive HCC tumor progression and sorafenib resistance by promoting cell proliferation, migration, and stopping apoptosis. Molecular mechanism findings demonstrated that the MEK/ERK signaling pathway activated the expression and activity of ETS-1 mediated by p-ERK, which led to its binding to the c-Met gene promoter and upregulation of c-Met transcriptional expression. The activation of the HGF/c-Met pathway drives sorafenib resistance in HCC cells by activating the Ras/Raf/ERK and PI3K/Akt signaling pathways, which regulate biologic processes, including cell proliferation, migration and anti-apoptosis. Conclusion: c-Met overexpression and activation is an essential mechanism of sorafenib resistance in HCC. Combination therapy of sorafenib plus c-Met inhibitor overcame the resistance of sorafenib-targeted therapy for HCC.

Keywords: Hepatocellular carcinoma, c-Met, sorafenib, sorafenib resistance, ETS-1

Introduction

Hepatocellular carcinoma (HCC) is the sixth commonest cancer worldwide and the third commonest cause of cancer fatality [1]; it accounts for 90% of primary liver cancers [2]. Risk factors for HCC include chronic hepatitis infection, aflatoxin exposure, smoking, and alcohol abuse. In areas with low hepatitis infection and aflatoxin exposure [3, 4], obesity, diabetes, and inappropriate diet and lifestyle habits also are important risk factors. Since HCC is often diagnosed at an advanced stage, only a minority of patients are eligible for palliative measures such as liver transplantation, resection, percutaneous ablation, transarterial chemoembolization, and radioembolization. Moreover, most patients with advanced HCC do not profit from conventional anti-tumor drugs. On the other hand, systemic therapies have been an option to prolong the survival of HCC patients for many years owing to the vigorous and widespread resistance to cytotoxic chemotherapy and the fact that HCC has never benefited in overall survival [5]. For HCC patients who have intermediate-to-advanced stage disease and are not suitable for local treatment, sorafenib, a multi-kinase inhibitor with anti-angiogenic and anti-proliferative properties, has been a first-line targeted HCC treatment since 2007 [6]. However, the effectiveness of sorafenib against cancer is unsatisfactory, since the drug only extends overall survival by about 3 months [7]. Another problem with sorafenib is that HCC cells acquire resistance to it, usually developing within 6 months in

patients who are initially sensitive to the drug [8]. Two clinical trials, the SHARP trial (in Europe and the United States) [9] and the Asia-Pacific study [10] (in the Asia-Pacific region), have shown that aberrant activation involved in epigenetic regulation, oxidative stress, and AKT-mTOR and MAPK signaling pathways is strongly associated with HCC progression and sorafenib resistance [11]. Increased c-Met and/or hepatocyte growth factor (HGF) expression in human tumor cells is usually associated with tumor progression and poor prognosis [12]; aberrant c-Met expression is associated with desensitization of HCC to anti-angiogenic agents, including sorafenib, regifenib, and cabozantinib [13]. Dysregulation of transcription factors in human cancer directly affects the expression level of this regulatory target gene [14]. Moreover, c-Met expression is mainly regulated at the transcriptional level. ETS-1 is an important transcription factor that activates the c-Met promoter and promotes the transcription and translation of c-Met [15]. Subsequently, aberrant activation of c-Met/HGF is associated with the development of HCC and resistance to sorafenib. c-Met, the HGF receptor, is a tyrosine kinase receptor with oncogenic properties. c-Met activation leads to phosphorylation of the receptor, resulting in recruitment of junctional proteins and activation of various signal transducers, including phosphatidylinositol 3-kinase (PI3K) and extracellular signal-regulated kinase (ERK)1/2, ultimately leading to stimulation of growth, survival, motility, and invasion in certain cell types [16]. c-Met is highly expressed in a variety of tumors, including esophageal, thyroid, metastatic melanoma, prostate, lung, and breast cancers [17].

In this study, we identified c-Met protein overexpression and activation as a key factor in the acquired resistance to sorafenib in HCC cell lines. Activation of the MAPK signaling pathway regulates c-Met transcription and expression by promoting the binding of the transcription factor ETS-1 to the c-Met promoter. Treatment of the sorafenib-resistant cell line Huh-7^R cells by a lentivirus interfering with c-Met expression and a specific inhibitor of c-Met, PHA-665752, revealed that downregulation of c-Met expression and activation inhibited the growth and migration of HCC Huh-7^R cells and restored their sensitivity to sorafenib.

Materials and methods

HCC tissue samples, cell lines, and cell cultures

Tissue samples were obtained from 20 HCC patients who had a good chemotherapeutic response to sorafenib and no disease progression and from 20 sorafenib-resistant patients whose disease progressed after sorafenib treatment. The study was approved by the ethics committee of the Medical School of Anhui University of Sciences and Technology. The study was conducted in accordance with the relevant guidelines formulated by the ethics review committee of the Medical School of Anhui University of Technology. Written informed consent was obtained from all patients before the samples were collected. All tissue samples were fixed in formalin and embedded in paraffin in compliance with the declaration of Helsinki. The human HCC cell lines Huh-7, SK-Hep1, HepG2, and human normal hepatocytes THLE-2 and HHL-5 were purchased from the American Type Culture Collection (Rockville, MD, USA). Huh-7^R (acquired sorafenib-resistant HCC cell line) was established from the Huh-7 cell line. When the cells were in logarithmic growth phase, the medium was changed, a lower concentration of sorafenib was added, and the cells were incubated for 24 h. Cell passages were performed, the stimulation was repeated at the same concentration of sorafenib, and the incubation was continued until stability was reached. The resistant cell line Huh-7^R was obtained when its resistance index was 4-5, and induction was terminated. Huh7 and Huh-7^R cells were cultured in RPMI-1640 (Gibco, Thermo Fisher Scientific Inc., Waltham, MA, USA) supplemented with 15% fetal bovine serum (Sijiqing Bioengineering Materials, Hangzhou, China). THLE-2 and HHL-5 were incubated in DMEM (Gibco, Thermo Fisher Scientific Inc., Waltham, MA, USA) containing 10% fetal bovine serum. SK-Hep1 and HepG2 were incubated in RPMI-1640 containing 10% fetal bovine serum. Cells were incubated at 37°C in 5% CO_2.

Reagents and antibodies

Sorafenib and PHA-665752 were purchased from MedChem Express (Monmouth Junction, NJ, USA). Recombinant human HGF was purchased from Peprotech (New York, USA). c-Met,

phospho-met (Tyr1349), phospho-ERK1/2 Kit (#9911), and ERK1/2, caspase-3, cleaved caspase-3, caspase-9, cleaved caspase-9, Akt, antibodies to phospho-Akt (Ser473), mTOR, phospho-mTOR (Ser2481), PI3K 110γ, Bim, β-actin, mTOR, phospho-mTOR (Ser2481), phospho-p70S6 kinase (Thr389), p70S6 kinase, and secondary horseradish peroxidase-coupled goat anti-rabbit and anti-mouse antibodies were purchased from Cell Signaling Technology (Danvers, MA, USA).

Wound-healing assay

Cells were cultured in RPMI 1640 containing 15% FBS in six-well plates. Cells in 80% confluent monolayers were scratched with a 10 μl pipette tip. Cells were washed twice with PBS to remove cell debris and cultured in RPMI 1640 culture medium without serum. After 24 h and 48 h, cells were observed for migration with phase contrast microscopy.

Immunochemical staining

Sections were dewaxed in xylene and hydrated. Immunostaining was performed with an automated immunohistochemical stainer according to the manufacturer's guidelines (Biogen, Lab vision autostainer 360). Antigen repair was assessed by treatment with proteinase K at 37°C for 20 min. Endogenous peroxidase activity was blocked by incubation with 3% H_2O_2 for 20 min at room temperature. Primary antibody against c-Met was applied and incubated at a dilution of 1:300. Sections were stained with 3, 3-diaminobenzidine tetrahydrochloride, chromogenic dye (brown), and restained with hematoxylin. Cells at a density of 3×10^5 cells/ml were incubated overnight on coverslips in 24-well plates. Crawls were removed and fixed in methanol, and endogenous peroxidase activity was blocked by incubation with a peroxide blocker for 30 min at room temperature. Goat serum was used to block nonspecific reactivity, and the cells were incubated overnight with anti-c-Met primary antibody. Crawls were stained with 3, 3-diaminobenzidine tetrahydrochloride and restained with hematoxylin. Images were acquired with a BX50 microscope (Olympus, Tokyo, Japan). Immunohistochemical positivity was quantified by scoring. 1,500 cells were examined and the number of cells with a significant signal was calculated. The positive score for each case was expressed as a percentage of positive cells relative to all cells. In each group, the mean and SD were calculated.

Western blotting

Total cellular proteins were extracted with SDS-PAGE and transferred to nitrocellulose PVDF membrane (IPVH00010, Millipore, USA). The following primary antibodies were used for immunoblotting: c-Met, Phospho-Met (Tyr13-49), Phospho-ERK1/2, ERK1/2, Caspase-3, Cleaved Caspase-3, Caspase-9, Cleaved Caspase-9, Akt, and phospho-Akt. Secondary antibodies were incubated for 1 h and exposed in electrochemiluminescence mode with a fully automated digital gel imaging system (Peiqing Science and Technology, Shanghai, China) with Image J software (Version 1.48) software (NIH, Bethesda, MD) to analyze the protein bands in grayscale value.

Immunofluorescence staining

Cells were inoculated overnight on circular slides in 24-well plates, washed with PBS, and fixed in 4% paraformaldehyde. After fixation, cells were washed with PBS, blocked with goat serum for 1 h, and incubated with anti-c-Met antibody at 4°C overnight. After being washed 3 times with PBS, cells were incubated with secondary antibody Alexa Fluor 488-coupled anti-rabbit IgG (A11070; Thermo Fisher Scientific Inc., Waltham, MA, USA) for 1 h and washed 3 times with PBS. Cell nuclei were restained with Hoechst33342 (C0078L-6, Beyotime, Jiangsu, China). Images were captured at magnification 200 with an inverted fluorescence microscope (Leica DMi8-M, Heidelberg, Germany).

Hematoxylin-eosin staining

Paraffin sections were dewaxed in ethanol to water in xylene, stained with hematoxylin for 5 min, fractionated with alcohol in hydrochloric acid for a few seconds, and rinsed with running water. Sections were stained in eosin solution for 1-3 min and dehydrated and sealed with neutral gum.

CCK-8 assay

Cell viability was measured with CCK-8 reagent. HCC cells (5,000 cells/well) were inoculated in 96-well plates and incubated with CCK-8 (Biomiky, Hefei, China) for 2 h. The cells were

incubated with CCK-8 (Biomiky, Hefei, China). The absorbance values at 450 nm were measured with an ELx800 (Bio-Tek, Winooski, VT, USA). All experiments were performed in triplicate.

Transwell assay

Transwell chambers (JET BIOFIL, Guangzhou, China) were used for cell migration assays. 3×10^5 HCC cells, resuspended in 100 μl RPMI 1640, were inoculated into the upper chamber. After 48 h incubation, the upper chamber membrane was fixed in methanol. Cells on the other side of the membrane were stained with crystal violet and photographed and counted under a microscope.

Clone formation assay

Six-well plates containing 1000 cells per well in 2 ml of cell culture solution were plated and treated with drugs, fixed in 4% paraformaldehyde after 10 days, stained with crystal violet, and counted.

Mitochondrial membrane potential (Δψm) JC-1 staining

JC-1 (Keygene Biotech, Nanjing, China) was dissolved with 1 ml of DMSO (Biofoxx, Germany) to a master mix concentration of 10 mg/ml. Cells were inoculated into 24-well plates at a final density of 1×10^5 cells per well. Cells were treated with the drug for 24 h, and 10 μg/ml of JC-1 in working concentration was added to each well and placed in the incubator at 37°C and 5% CO_2 for half an hour. Finally, the wells were stained with Hoechst 33342 for 10 min. Inverted fluorescence microscopy was used to detect changes in mitochondrial membrane potential.

Acridine orange/ethidium bromide (AO/EB) double staining

Dual fluorescence staining solution containing 100 μg/ml acridine orange (AO) (Solarbio, Beijing, China) and ethidium bromide (EB) (Keygene Biotech, Nanjing, China) were mixed and added to 100 μl PBS, mixed, and transferred onto cell crawl sheets. The morphology of apoptotic cells was observed and counted with an inverted fluorescence microscope. The percentage of apoptotic cells = (total number of apoptotic cells/total number of cells counted) ×100%.

5-ethynyl-2'-deoxyuridine staining

3×10^5 HCC cells were inoculated into 24-well plates. After each group was treated with medication, proliferating cells were quantified based on 5-ethynyl-2'-deoxyuridine (EdU) incorporation of DNA with the BeyoClick™ EdU-594 in vitro imaging kit (Beyotime Biotechnology, Shanghai, China). Cells were counted under an inverted microscope.

Lentivirus transfection

Huh-7^R cells were inoculated in 6-well plates and cultured for 24 h. Cells were treated with polybreen (5 μg/mL) and infected with pLVE3164 carrying c-Met siRNA and control lentivirus (Sangon Biotech, Shanghai, China), respectively. Total cellular proteins were extracted after transfection at 72 h. The expression of c-Met in the transfected Huh-7^R cells was determined by immunoprotein blotting.

Adenovirus infection

Adenoviral overexpression vector construction and packaging of the human c-Met gene was performed by Sangon Biotech, Shanghai, China. Huh-7 cells were incubated with the corresponding volume of adenovirus in 1/2 volume of culture medium for 4 h. After infection, the medium was replaced with fresh, complete medium and incubated for 72 h, then stimulated with drugs or directly harvested.

Chromosomal immunoprecipitation assay

The binding of ETS-1 to the c-Met promoter was corroborated by chromosomal immunoprecipitation (ChIP) assay with a kit (Thermo Fisher Scientific Inc., Waltham, MA, USA) in accordance with the manufacturer's guidelines. One percent formaldehyde was added into cultured Huh-7^R cells to produce cross-linked protein and DNA. Chromatin fragments were made through sonication with a Bioruptor (Diagenode SA). An antibody against ETS-1 was used for immunoprecipitation with normal IgG as control (Santa Cruz, USA). The recuperated DNA fragments were evaluated via reverse transcription-quantitative polymerase chain reaction (RT-qPCR).

Reverse transcription-PCR (RT-PCR)

Total RNA was extracted with TRIzol Reagent (Sangon Biotech, Shanghai, China). PCR was

performed with the RT-PCR Kit (Takara, Japan) with 5 μg total RNA to synthesize cDNA. The primers of c-Met were 5'-TGAACGCTACTTATG-TGAAC-3' (forward primer) and 5'-TGTCCACCT-CATCATCAG-3' (reverse primer). The primers of ETS-1 were 5'-TACACAGGCAGTGGACCAATC-3' (forward primer) and 5'-CCCCGCTGTCTTGTGG-ATG-3' (reverse primer). β-actin was used as an internal control. The primers of β-actin were 5'-CATGTACGTTGCTATCCAGGC-3' (forward primer) and 5'-CTCCTTAATGTCACGCACGAT-3' (reverse primer). PCR was performed in 30 μL of reaction mixture. Thermal cycles were conducted with preamplification denaturation at 95°C for 3 min, followed by 30 cycles of denaturation at 95°C for 20 s, annealing at 56°C for 20 s, and extension at 72°C for 30 s, with a final extension at 72°C for 3 min. For the semi-quantification, an image of the gel was captured, and the intensity of the bands was quantified by a gel analysis system (Bio-Rad, USA).

Xeno-transplantation assay

BALB/c thymus-free female nude mice (4-6 weeks old) were purchased from Nanjing Junke Bioengineering Co., Ltd. (Nanjing, China). Each experimental group consisted of 10 mice. The mice were raised in a pathogen-free environment at the Laboratory Animal Center in the Medical School of Anhui University of Science and Technology. All animal experiments were approved by the ethics committee of the Medical School of Anhui University of Science and Technology. All experimental procedures involving animals were carried out in accordance with guidelines formulated by the ethics review committee of the medical school of Anhui University of Technology. The study was also conducted in accordance with the ARRIVE guidelines. At the end of the experiment, all mice were euthanized with excessive ether. Huh-7^R cells were transfected with pLVE3164, and cells were collected after 72 h. Huh-7^R cells were also collected and resuspended in PBS phosphate buffer, and 1×10^6 cells were injected into the right axilla of each mouse. Four xenograft tumor models were established: blank control group (PBS), sorafenib group (30 mg/kg), sorafenib combined with inhibitor PHA665752 group (30 mg/kg + 25 mg/kg) and pLVE3164 + sorafenib group (30 mg/kg). Every three days, the tumor volumes were measured, and the tumors were weighed. The volume was calculated according to the formula (long diameter × wide diameter^2)/2. Mice were euthanized after 30 days of monitoring, and tumor tissues from each group were harvested and homogenized in protein lysis buffer to prepare whole-cell protein lysates for protein blotting assays for further analysis.

Statistical data

Data were obtained in triplicate. Measured values were expressed as mean values ± standard deviation. Data were analyzed with SPSS 18.0 software (SPSS Inc., Chicago, IL, USA) and Prism 5 (GraphPad, La Jolla, CA, USA) software. Analysis of variance (ANOVA) tests were used to compare means between three or more groups, and t-tests were used to compare two sets of data with normal distribution. Statistical significance was set at $P<.05$.

Results

c-Met was overexpressed in tissues and cells of sorafenib-resistant HCC

We investigated the expression of c-Met in samples from patients with HCC resistant to sorafenib or HCC patients well treated with sorafenib. The expression levels of c-Met were analyzed with immunohistochemistry. Sorafenib-resistant HCC samples had overexpressed of c-Met, which was higher than in samples from HCC patients who were well treated with sorafenib (P<.001) (**Figure 1A**, **1B**). This result is consistent with c-Met being present in the cell membrane and cytoplasm. To obtain a sorafenib-resistant HCC cell line, the Huh-7 cell line was treated with sorafenib at progressively increasing concentrations. The CCK-8 assay was applied to determine whether HCC sorafenib-resistant cells were established. IC_{50} values of sorafenib against Huh-7 and Huh-7^R were determined. The resistance index RI = IC_{50} of resistant cells/IC_{50} of parental cells was determined. RI was 4.89 (**Figure 1C**), indicating that a resistant strain had been established. The cell line Huh-7 was characterized as well-differentiated, as the western blotting assay showed that c-Met was expressed at low levels in Huh-7 cells, whereas expression was significantly higher in Huh-7^R cells ($P<.05$) (**Figure 1D**, **1E**). The results of immunocytochemistry and indirect immunofluorescence assays also showed that the expression levels of c-Met molecules were significantly higher in Huh-7^R cells than in Huh-7 cells (**Figure 1F**, **1I**). Also, when Huh-7 and Huh-7^R cells were treated with the

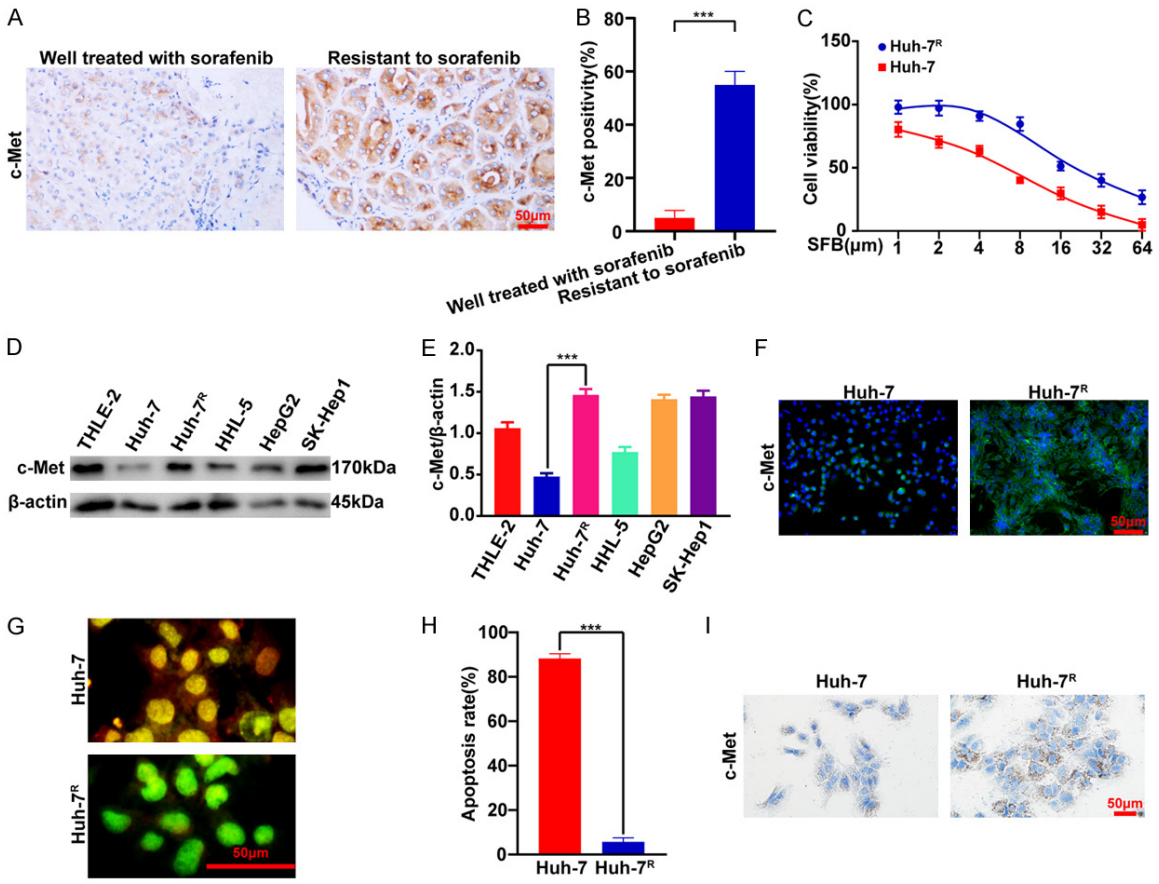

Figure 1. c-Met is overexpressed in tissues and cells of sorafenib-resistant HCC. A, B. Immunohistochemical analysis of c-Met expression was performed on tissue sections of HCC patients well treated with sorafenib and resistant to sorafenib was conducted on the tissue sections. Representative images were selected to present. C. Huh-7 and Huh-7^R cells were treated with various concentrations of sorafenib for 24 h, and the IC_{50} values of the two cell lines to sorafenib were determined with CCK-8 assay. D, E. Western blotting was carried out to detect c-Met expression in HCC cell lines. The c-Met expression levels of HCC cell lines relative to β-actin were quantified with Image J software analysis. F. Indirect immunofluorescence staining results of c-Met in Huh-7 and Huh-7^R were taken at 200× with inverted fluorescence microscopy. G, H. The apoptosis rates of Huh-7 and Huh-7^R after 24 h treatment with the same concentration of sorafenib were detected with acridine orange/ethidium bromide (AO/EB) assay. Images were taken with an inverted fluorescence microscope at 200×. Scale bar: 50 μm. I. c-Met immunocytochemical staining in Huh-7 and Huh-7^R were photographed at 400× magnification with an ortho-fluorescence microscope. Representative images from three experiments are displayed. (Mean ± SD; n=3; **P*<0.05, ***P*<0.01 and ****P*<0.001).

same concentration of sorafenib, the apoptosis ratio of Huh-7^R cells was significantly lower than that of the parental cell line Huh-7 cells (**Figure 1G**, **1H**). Therefore, c-Met high level (Huh-7^R) cells and c-Met low level (Huh-7) cells were selected for further study.

The MAPK signaling pathway promotes the binding of ETS-1 to the c-Met gene promoter and upregulates the transcriptional expression of c-Met

ETS-1 is an essential transcription factor that activates the c-Met promoter. Therefore, RT-PCR and western blotting were used to detect the expression of c-Met and ETS-1. The correlation between ETS-1 protein expression levels and c-Met mRNA levels was examined using two human normal hepatocyte cell lines and three HCC cell lines. Although these cell lines differed in mRNA and protein expression levels of c-Met, mRNA and protein levels were correlated (R^2=0.966; **Figure 2A**, **2B**). In addition, c-Met mRNA levels and ETS-1 protein levels were correlated (R^2=0.892; **Figure 2A**, **2C**). The two correlations were statistically different. Two ETS-1 binding sites (S1 and S2) on the c-Met promoter region were predicted by consulting the JASPAR database (http://jaspar.genereg.net/) (**Figure 2D**). To further determine the

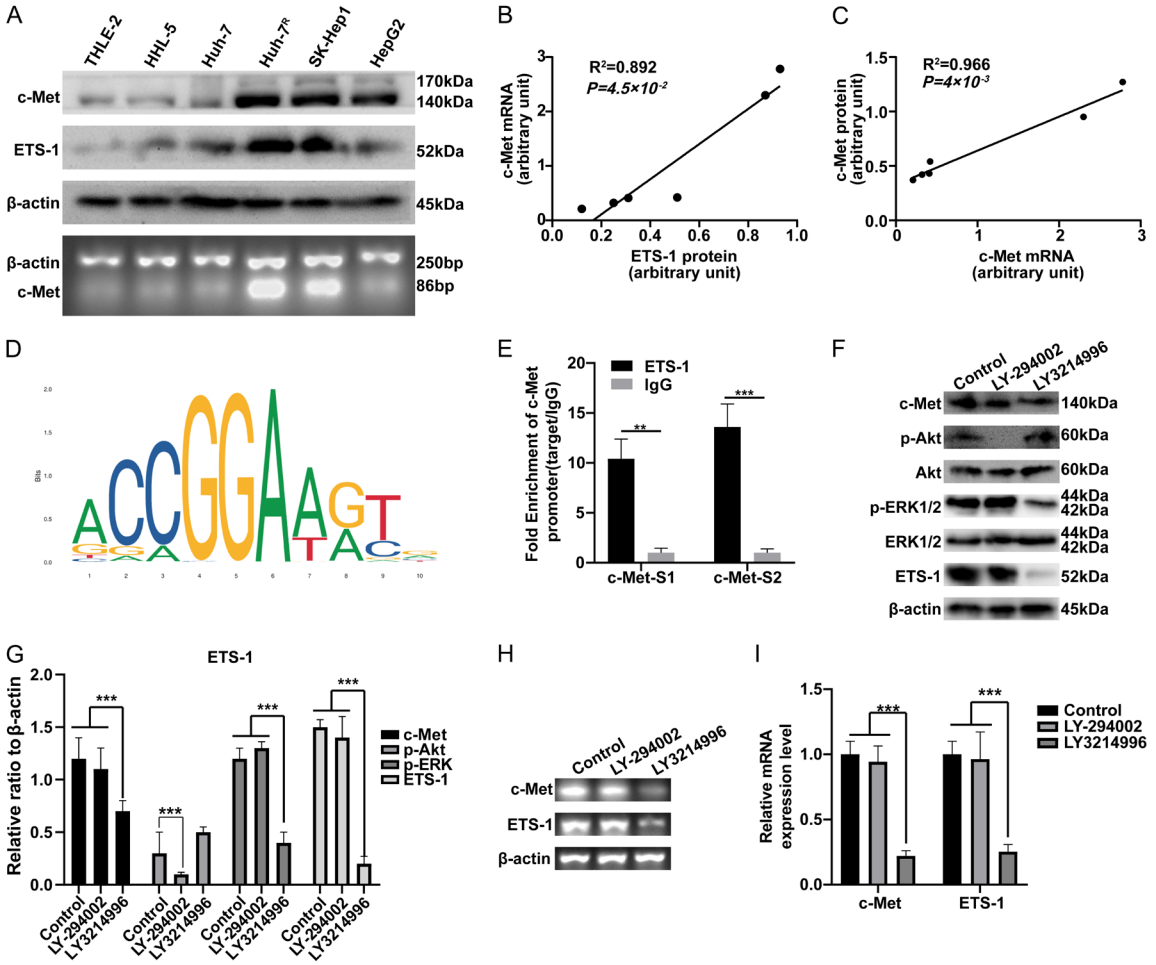

Figure 2. MAPK signaling pathway promotes the binding of ETS-1 to the c-Met gene promoter and upregulates the transcriptional expression of c-Met. (A) The levels of c-Met protein, c-Met mRNA and ETS-1 protein were determined by western blotting or RT-PCR, as described in Material and Methods. (B, C) The image of each result is shown in (A). After quantification, the correlation between c-Met mRNA and ETS-1 protein levels and that between c-Met protein and c-Met mRNA levels were statistically examined. (D) ETS-1 sequence and binding sites to c-Met promoter region were predicted by using JASPAR database (http://jaspar.genereg.net/). (E) ChIP assays were performed to confirm the direct binding of ETS-1 to c-Met promoter in Huh-7^{R} cells. ChIP analysis was performed using a negative control immunoglobulin G (IgG) or anti-ETS-1 antibody in Huh-7^{R} cells. (F, G) Western blotting was performed to analyze the effect of MAPK and PI3K inhibitor (LY3214996 and LY-294002) on the expression levels of key molecules. (H, I) RT-PCR was conducted to analyze the effects of MAPK and PI3K inhibitors (LY3214996 and LY-294002) treatment on c-Met and ETS-1 mRNA levels. Data are presented as mean ± SD from three independent experiments. *P<0.05, **P<0.01 and ***P<0.001.

binding of ETS-1 to the c-Met promoter, ChIP analysis was conducted; the ETS-1 antibody significantly recruited fragments of transcription factor binding site (TFBS) S1 and S2 (**Figure 2E**). These results suggest that, as a transcription factor, ETS-1 binds directly to the promoter of c-Met. To determine which downstream signaling pathway is involved in upregulating ETS-1 and thus enhancing c-Met transcription and expression, cells were treated with inhibitors of MAPK and PI3K LY3214996 and LY-294002, respectively. Whole lysates from cells were analyzed with western blotting, and RT-PCR was applied to detect the mRNA levels of c-Met and ETS-1. **Figure 2F** and **2G** illustrate that LY3214996 blocked the activity of p-ERK and decreased the mRNA levels of ETS-1 (**Figure 2H**, **2I**) and subsequently downregulated the expression of ETS-1; however, LY-294002 had no effect on ETS-1 transcription and expression, suggesting that activation of ETS-1 requires MAPK signaling rather than PI3K/AKT signaling. Our data further indicated that ETS-1 is located downstream of the MAPK signaling

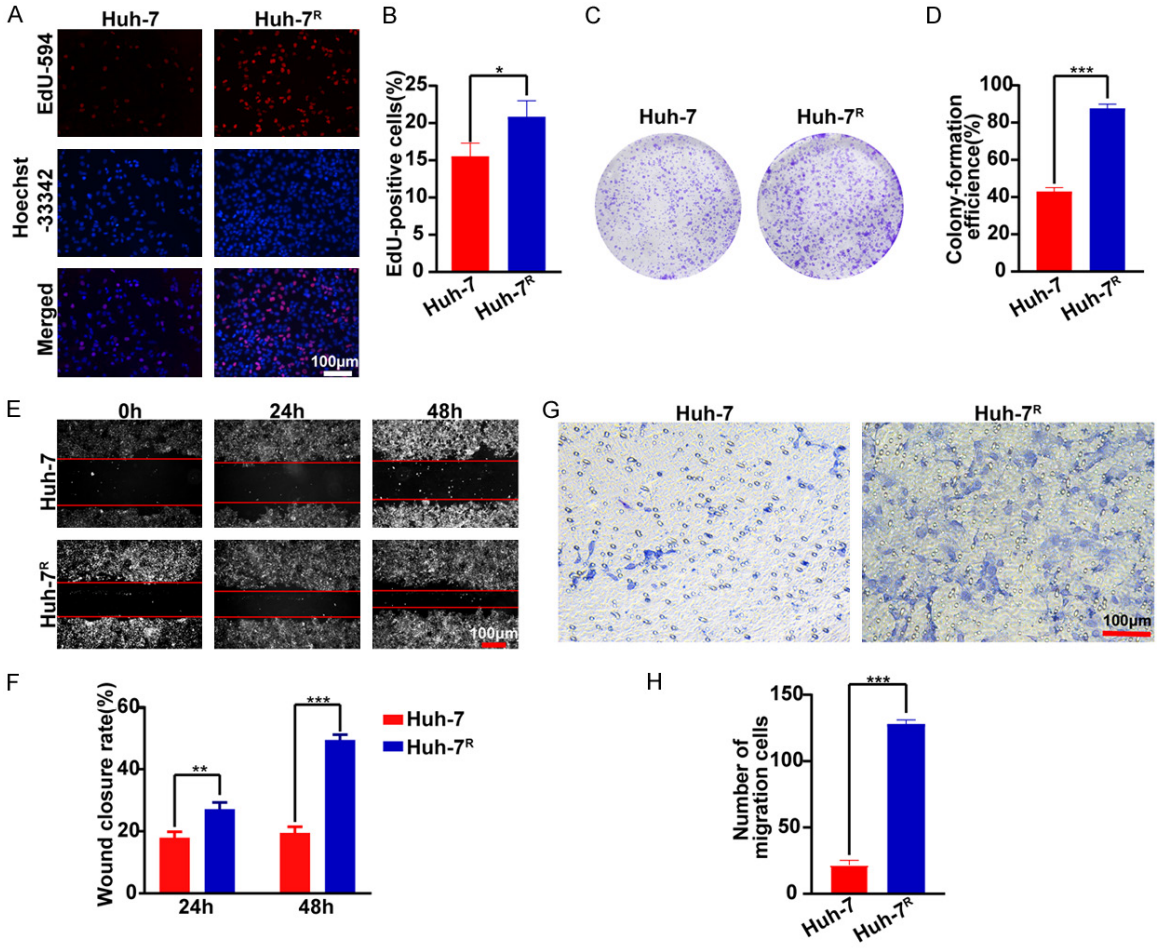

Figure 3. The migration and proliferation of Huh-7^R cells overexpressed with c-Met were enhanced. A-D. After 50 ng/ml HGF treatment of Huh-7 and Huh-7^R for 24 h and 10 days, respectively, the effects of short-term and long-term HGF interaction on the proliferation rate of both cell lines were examined with EdU and cell clone formation assays. Scale bars: 100 μm. Representative images from three experiments are displayed. E, F. Huh-7 and its resistant strain Huh-7^R were treated with 50 ng/ml HGF for 24 h and 48 h, respectively, then scratch healing rate was detected with cell scratch assay. G, H. Equal amounts of cells were added to transwell chambers, and crystalline violet staining was performed to count migrated cells after 48 h. Images were photographed at 400× magnification. Data are presented as mean ± SD from three independent experiments. *P<0.05, **P<0.01 and ***P<0.001.

pathway and is activated to bind to the c-Met gene promoter and then upregulates the transcription and expression of c-Met.

The migration and proliferation of Huh-7^R cells overexpressed with c-Met were increased

To determine the proliferative capacity of the Huh-7 cells and drug-resistant Huh-7^R cells we treated the cells with HGF at the same concentrations. In experiments on the proliferative capacity with EdU-594, the proliferation rate of Huh-7^R cells overexpressing c-Met was significantly greater than in those without overexpression (**Figure 3A**, **3B**). Consistently, long-term cell clonogenesis assays also showed that the clonogenesis rate of Huh-7^R cells was significantly more than that of Huh-7 cells (**Figure 3C**, **3D**). Further, we applied the cell scratch assay to analyze the migration properties of the cells, as shown in **Figure 3E**, **3F**. The scratch healing rate of c-Met low- expressing parental Huh-7 cells treated with HGF for 24 h and 48 h was not significantly increased compared with the rate in the untreated group, whereas the rate was significantly more in Huh-7^R cells after 24 h and 48 h (P<.001) (**Figure 3E**, **3F**). We further examined the migration rate of Huh-7 and Huh-7^R cells in Transwell assay; the migration of Huh-7^R cells was significantly more than that of the Huh-7 cell line cells (**Figure 3G**, **3H**).

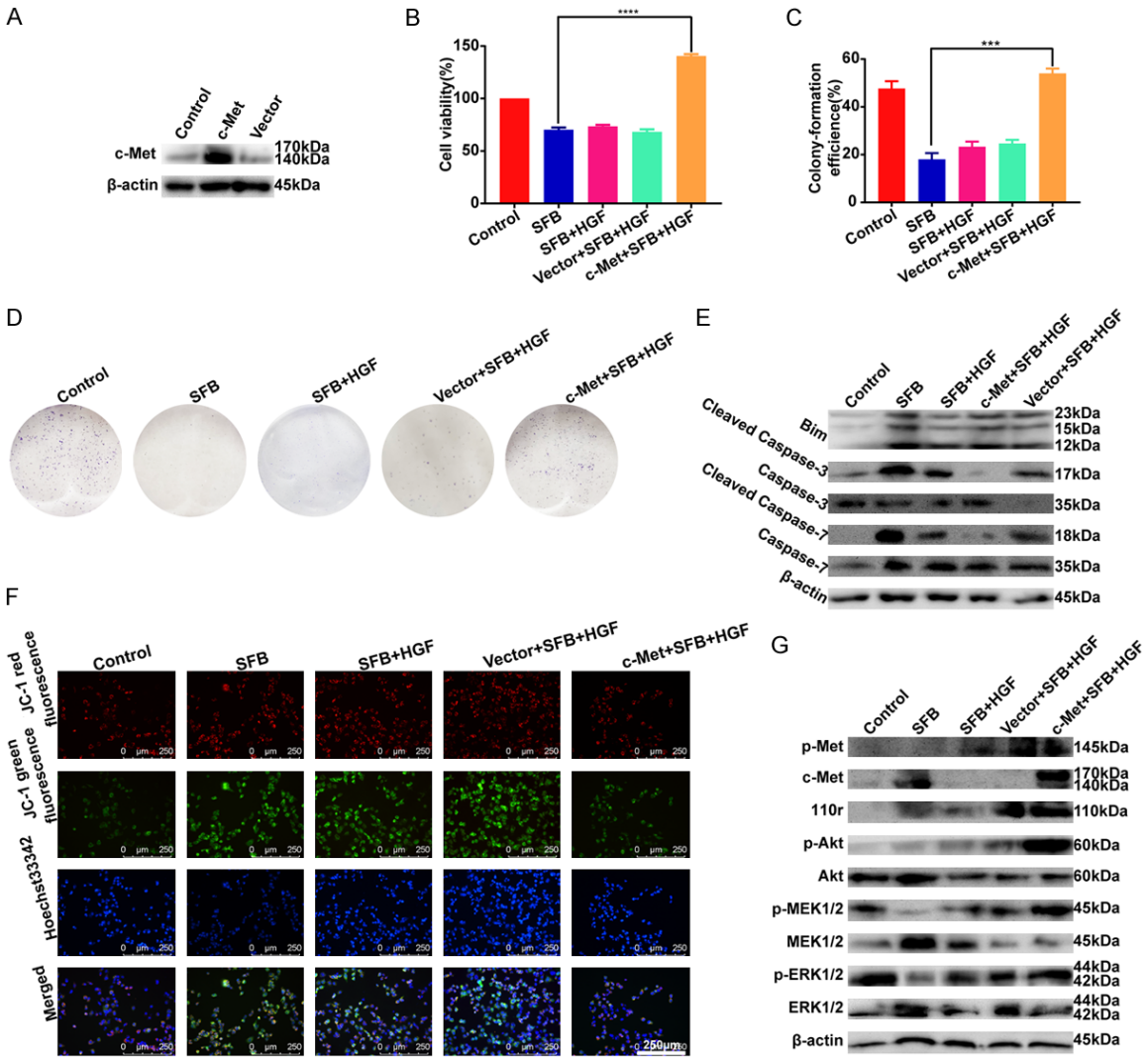

Figure 4. Huh-7 cells with c-Met overexpression induce desensitization to sorafenib and activation of PI3K/Akt and MAPK signaling pathways. A. The c-Met expression levels of the parental strain, Vector group (transfected control adenovirus group) and c-Met group (transfected high c-Met expressing adenovirus group) were measured with western blotting. B. Cell viability of each cell line was detected with CCK-8 assay after 24-h treatment with various drugs. C, D. After transfection with the corresponding adenovirus, equal amounts of cells were added to each well, treated with various compounds for 7 days, and photographed and counted after crystalline violet staining. E. Immunoblotting to detect the expression levels of mitochondrial apoptotic molecules in the parental strain. Vector group (transfected with control adenovirus group) and c-Met group (transfected with high expression c-Met adenovirus group) after treatment with different groups of compounds are illustrated. F. JC-1 staining was assayed for changes in mitochondrial membrane potential in the treatment groups. G. The activation levels of key molecules of two signaling pathways activated by HGF/c-Met were detected after drug treatment. Data are presented as mean ± SD from three independent experiments. SFB: sorafenib. **P*<0.05, ***P*<0.01 and ****P*<0.001.

Huh-7 cells with c-Met overexpression induce desensitization to sorafenib and activation of PI3K/Akt and MAPK signaling pathways

After transfection of c-Met overexpressing adenovirus (c-Met) and control adenovirus (Vector) in Huh-7 cells, total cell protein was extracted after 72 h. The results of protein immunoblotting showed that c-Met was significantly overexpressed in Huh-7 cells transfected with c-Met overexpressing adenovirus (Huh-7$^{\text{c-Met}}$) (**Figure 4A**). The absorbance values of drug-treated groups were read with CCK-8 assay, and the corresponding cell viability of each group was obtained after 24 h. The difference in cell viability between Huh-7$^{\text{c-Met}}$ and parental cell lines treated with the same concentration of sorafenib was significant (*P*<.001), and Huh-

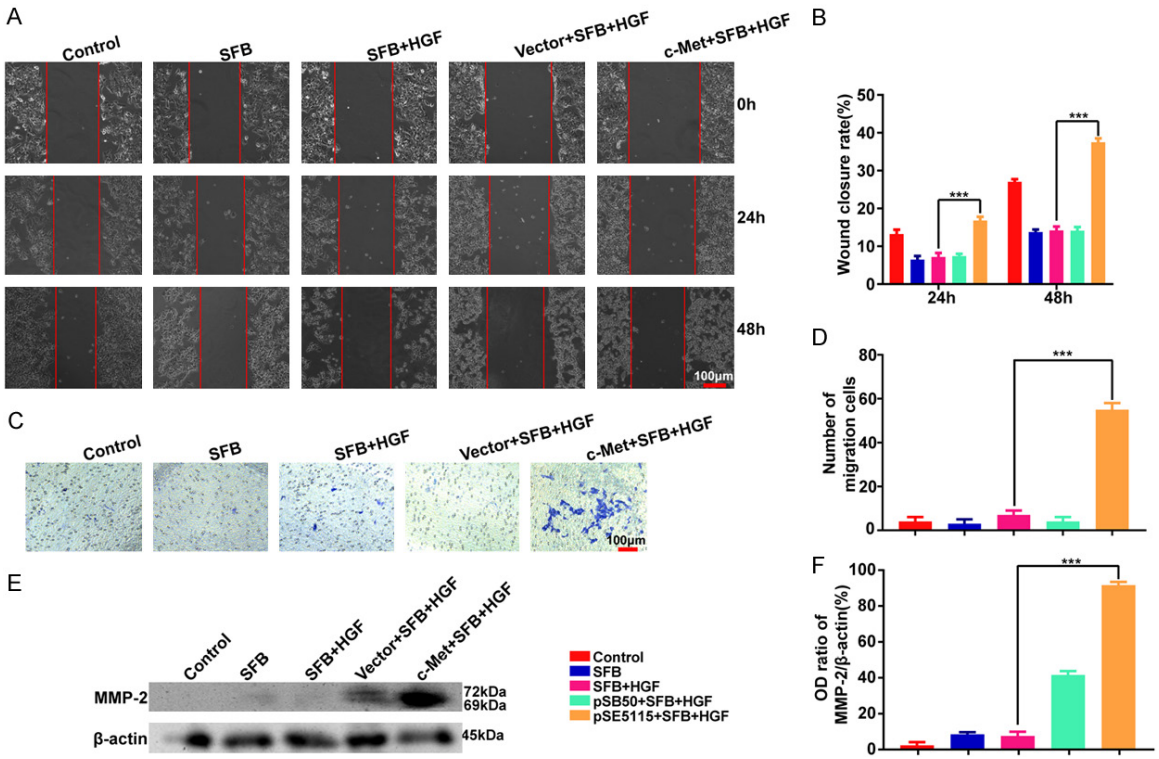

Figure 5. Migratory ability of Huh-7 cells with c-Met overexpression is significantly enhanced. A, B. Cell scratch assay was performed to evaluate the scratch healing ability of cell lines in treatment groups at 24 h and 48 h. C, D. Transwell assay was performed to analyze the number of perforated cells in each treatment group after 48 h. E, F. Western blotting was conducted to evaluate the expression level of migration-associated protein molecule MMP-2 in treatment groups. Images were photographed at 400× magnification. **P*<0.05, ***P*<0.01 and ****P*<0.001.

$7^{\text{-c-Met}}$ lost sensitivity to sorafenib after HGF treatment (**Figure 4B**).

The results of the clone formation assay also suggested that Huh-$7^{\text{-c-Met}}$ lost susceptibility to sorafenib (**Figure 4C**, **4D**). We applied immunocytoblotting to detect the levels of mitochondrial apoptosis-related molecules in each treatment group. Among them, the pro-apoptotic molecule Bim was significantly down-regulated, and the cleaved Caspase-3 and -7 were present at low levels (**Figure 4E**). In the clone formation assay, the mitochondrial membrane potential (ΔΨm) in normal cells is high, and JC-1 aggregates in the mitochondrial matrix form polymers that produce red fluorescence; however, when apoptosis occurs, the mitochondrial transmembrane potential is depolarized, and JC-1 fluoresces green as a monomer dispersed in the cytoplasm. In these experiments, we found that Huh-$7^{\text{-c-Met}}$ exhibited reduced green fluorescence after treatment with sorafenib and HGF compared with cells treated with sorafenib alone (**Figure 4F**). Also, Huh-$7^{\text{-c-Met}}$ treated with HGF activated c-Met, rescued the inhibition of p-MEK1/2, p-ERK1/2 by sorafenib, and upregulated the expression of 110γ and the level of p-Akt, indicating activation of the PI3K/Akt, MAPK signaling pathway (**Figure 4G**).

Migratory ability of Huh-7 cells with c-Met overexpression is significantly enhanced

After Huh-$7^{\text{-c-Met}}$ cells were treated with the corresponding compounds, as indicated, for 24 h and 48 h, the results of scratch healing rates showed that Huh-$7^{\text{-c-Met}}$ had significantly enhanced migration ability compared to that of Huh-$7^{\text{-Vector}}$ (Huh-7 cells transfected with control adenovirus Vector) and parental cells (**Figure 5A**, **5B**). Similar results were found in the Transwell assay (**Figure 5C**, **5D**). The migration-associated protein MMP-2 was correspondingly highly expressed in Huh-$7^{\text{-c-Met}}$ (**Figure 5E**, **5F**). These results suggest that c-Met overexpression enhances the migratory ability of HCC cells.

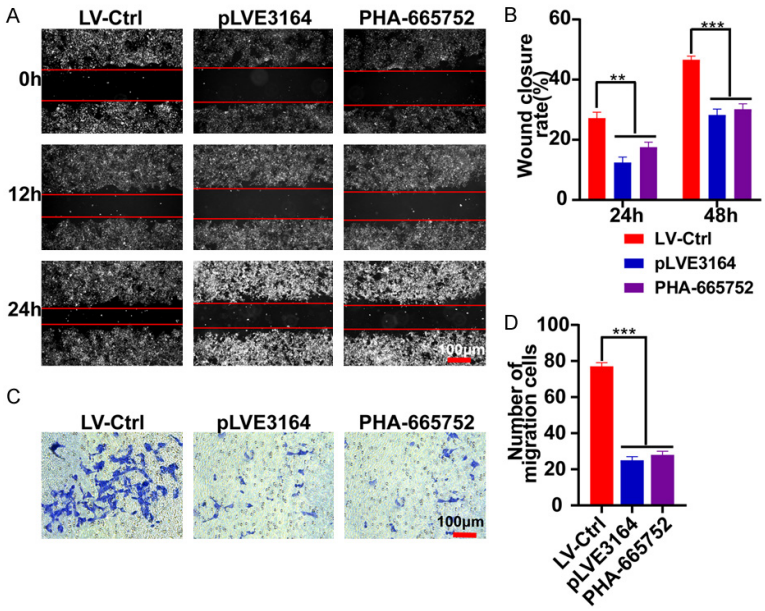

Figure 6. Knockdown of c-Met or inhibition of c-Met activity reduces the migration ability of Huh-7^{R} cells. A, B. Huh7^{R} cells were transfected with negative control lentivirus (LV-Ctrl) or lentivirus expressing siRNA targeting c-Met (pLVE3164). Cell scratch assay was performed to analyze the scratch healing ability of the three experimental groups at 0 h, 24 h, and 48 h. C, D. Transwell assay measured the number of cell perforations in the three treatment groups, reflecting their migration ability. Images were photographed at 400× magnification. Data are represented as the mean ± SD from three independent experiments. *P<0.05, **P<0.01 and ***P<0.001.

Knockdown of c-Met or inhibition of c-Met activity reduces the migratory ability of Huh-7^{R} cells

Huh-7^{R} transfected with control adenovirus (LV-Ctrl) and knockdown c-Met lentivirus (pLVE3164) were pre-treated with 50 ng/ml of HGF for 24 h. Huh-7$^{R\text{-LV-Ctrl}}$ and Huh-7$^{R\text{-pLVE3164}}$ were not additionally treated, but the Huh-7^{R} group was treated with the c-Met inhibitor PHA-665752; the scratch migration images were captured after 0 h, 24 h, and 48 h. Compared to the control adenovirus group, the migration rate at 24 h and 48 h was significantly lower in the c-Met knockdown group and the group that had blocking c-Met activation with PHA-665752 (**Figure 6A**, **6B**). Transwell analysis of the 48 h-migrating cell numbers in the three groups also revealed that reducing c-Met expression and activation in Huh-7^{R} cells inhibited the migration of HCC cells (**Figure 6C**, **6D**).

Inhibition of c-Met expression and activation reversed the acquired resistance of Huh-7^{R} cells to sorafenib

Transfected control adenovirus LV-Ctrl, knockdown c-Met expression adenovirus pLVE3164, and Huh-7^{R} pre-treated with c-Met inhibitor PHA-665752 for 6 h were simultaneously treated with 50 ng/ml of HGF for 1 h. The c-Met expression and activation levels were detected by western blotting. The results revealed that pLVE3164 adenovirus significantly decreased c-Met expression, and the level of phosphorylated c-Met, a marker of c-Met activity, was significantly decreased in the Huh-7$^{R\text{-pLVE3164}}$ and PHA-665752 groups compared with the level in the Huh-7$^{R\text{-LV-Ctrl}}$ group (**Figure 7A**, **7B**). When the expression and activation levels of c-Met of Huh-7^{R} were downregulated, the clonal proliferation of its long-term individual cells was also significantly downregulated (**Figure 7C**, **7D**). EdU insertion into DNA molecules undergoing replication, reflecting changes in the proliferation rate at the molecular level, caused the same reduction in proliferation rate (**Figure 7E**, **7F**). Also, as shown in **Figure 7F**, **7G**, treatment with the same concentration of sorafenib significantly increased the apoptosis rate in the other two groups compared to the rate in LV-Ctrl, thus enhancing the cytotoxic effect of sorafenib on Huh-7^{R} (**Figure 7G**, **7H**). To explore the effect of c-Met in sorafenib resistance in HCC cells, we also investigated the sensitivity of Huh-7^{R} cells to sorafenib. The half-inhibitory concentration (IC_{50}) values of sorafenib decreased with decreasing activation levels of c-Met expression. Thus, c-Met expression, activation, and sorafenib resistance in HCC cells were positively correlated (**Figure 7I**). Western blotting analysis showed that c-Met overexpression and activation increased the levels of p-ERK1/2 and

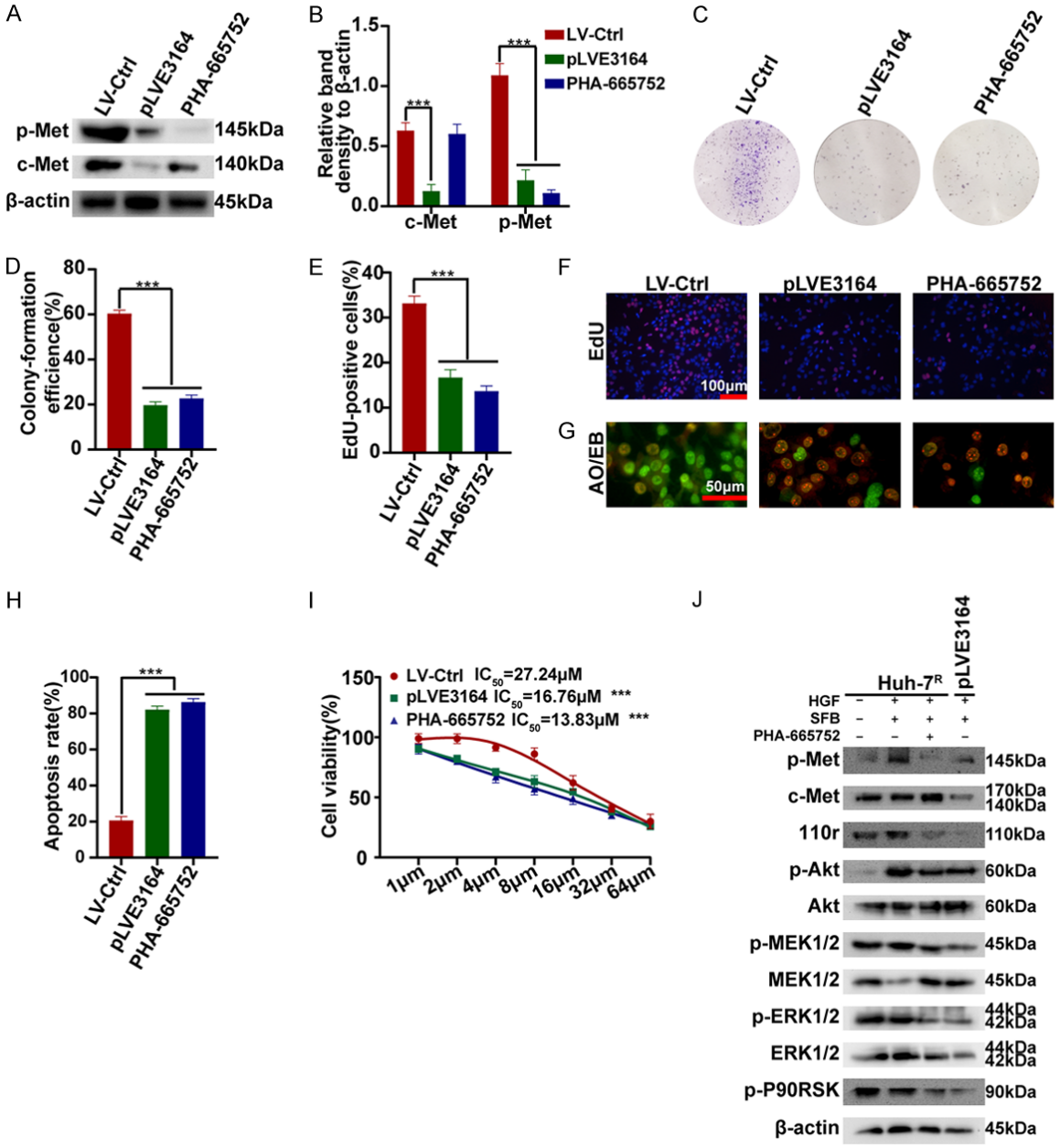

Figure 7. Inhibition of c-Met expression and activation reversed acquired resistance of Huh-7^R cells to sorafenib. A, B. Western blot was analyzed for changes in basal and activation levels of c-Met after treatment of pLVE3164, PHA-665752 with Huh-7^R. C, D. The clone formation rate was analyzed with crystalline violet staining after 24 h of HGF pre-treatment with or without the addition of PHA-665752 for 10-days. E, F. The nucleic acid molecular labeling technique EdU was used to detect changes in cell proliferation rate. Blue color represents the nucleus and purple color indicates the cells undergoing proliferation. G, H. AO/EB staining was performed to measure the change in apoptosis rate after treatment with a medicine (representative images from three experiments). I. Cells transfected with control lentivirus LV-Ctrl or lentivirus pLVE3164 and cells treated with c-Met inhibitor PHA-665752 were subjected to CCK-8 assay to detect the effect of sorafenib on cell viability of the three groups of cells and to analyze the IC_{50} variability. J. Western blotting was performed to detect the expression levels of HGF/c-Met, PI3K/Akt, and key kinases of the MAPK signaling pathway. Images were photographed at 400× magnification. *P<0.05, **P<0.01 and ***P<0.001.

p-Akt proteins as well as the MAPK downstream protein p-P90RSK. These findings suggest that HGF/c-Met signaling pathway activation promotes sorafenib resistance in HCC cells by pro-

moting PI3K/Akt and MAPK signaling. To rigorously demonstrate that HGF/c-Met activates PI3K/Akt and MAPK signaling pathways, we used the specific c-Met inhibitor PHA-665752 as well as pLVE3164 to verify the effects on PI3K/Akt and MAPK pathways. Western blot results revealed that in Huh-7^{R} cells compared with the LV-Ctrl group, the upregulation of PI3K/Akt and MAPK signaling pathways was significantly reversed in the pLVE3164 and PHA-665752 groups compared with that in the LV-Ctrl group; this finding documented that the PI3K/Akt and MAPK pathways are key links in the induction of sorafenib resistance in Huh-7^{R} cells by HGF/c-Met (**Figure 7J**).

Enhanced antitumor activity of sorafenib by inhibition of the expression and activation of c-Met in vivo

We next conducted experiments to determine whether c-Met has a role in promoting tumor growth in vivo by modulating sorafenib resistance. Huh-7$^{R\text{-}pLVE3164}$ cells and their corresponding Huh-7^{R} were subcutaneously inoculated into BALB/c nude mice. As shown in **Figure 8A** and **8B**, tumorigenicity and growth rate were significantly lower in the Huh-7$^{R\text{-}pLVE3164}$ group than in the control group and the group treated with sorafenib alone. The nude mice were tolerant to each drug or their combination, as there was not a significant reduction in body weight of the mice during treatment (**Figure 8C**). Changes in the level of activation of intrinsic protein molecule expression were analyzed by western blotting (**Figure 8D** and **8E**). Consistent with the in vitro results, c-Met activation within the xenografts of Huh-7^{R} cells with high c-Met expression and the downstream PI3K/Akt and MAPK signaling pathways were also activated; in contrast, after c-Met knockdown, the pathways were all downregulated. The combination of PHA-667552 and sorafenib inhibited PI3K/Akt, and MAPK activation induced by HGF/c-Met activation, and downregulated p-p70S6K and p-p90RSK activation (**Figure 8D** and **8E**). As shown in **Figure 8F**, the expression of c-Met in the pLVE3164 group was significantly lower than in the other three groups. In addition, the expression of p-Met in the pLVE3164 group and the combined group was significantly lower than in the other two groups. The results of the Ki67 experiment showed that the proliferation level of the pLVE3164 group and the combined group was decreased significantly (**Figure 8G**). These findings imply that c-Met mediates the resistance of HCC to sorafenib treatment and promotes tumor growth in HCC.

Discussion

Systemic therapy is the preferred treatment for patients with advanced HCC, and the first-generation targeted therapy, sorafenib, has been beneficial for this population [7]. Unfortunately, the treatment is associated with severe side effects, and the survival benefit for most patients is limited to 3-5 months, mainly because of the development of resistance to sorafenib. Aberrant tyrosine kinase receptor expression and feedback activation and/or crosstalk activation of key signaling pathways, such as Ras/Raf/MEK/ERK, PI3K/Akt, HGF/c-Met, Wnt, and Hedgehog, are important in inducing resistance to sorafenib [18]. c-Met overexpression and activation increases proliferation, survival, migration, and invasiveness of cancer cells [16]. Aberrant activation of the HGF/c-Met axis is often present in solid tumors and plays a key role in malignant transformation by promoting tumor-cell migration, epithelial mesenchymal-transformation, and invasion [19]. c-Met expression regulatory pathways have been found activated through gene mutations, gene amplification, increased receptor expression levels, or signaling pathway crosstalk in HCC tissues from 20% to 50% of patients [20]. In our work with HCC cells, cellular immunochemical assays revealed that the sorafenib-resistant cell line Huh-7^{R} was highly expressed c-Met (**Figure 1**), which suggests that sorafenib induces the expression of c-Met molecules in HCC and that abnormal c-Met is associated with resistance to sorafenib. Transcription factors are proteins that bind to DNA and control the rate of transcription of a set of genes; they are some of the most important regulators of gene expression. Cells are largely influenced by the controlling effects of transcription factors, which recognize and bind specific sequences in the genome to regulate gene expression [21]. In this study, we used a bioinformatic approach to predict the relevant transcription factors that regulate c-Met transcriptional expression, which was targeted on transcription factor ETS-1 by predicted scoring levels and reference to relevant literature. The presence of the predicted site was verified by ChIP-qPCR, and the results showed that the transcription factor ETS-1 bound to both sites

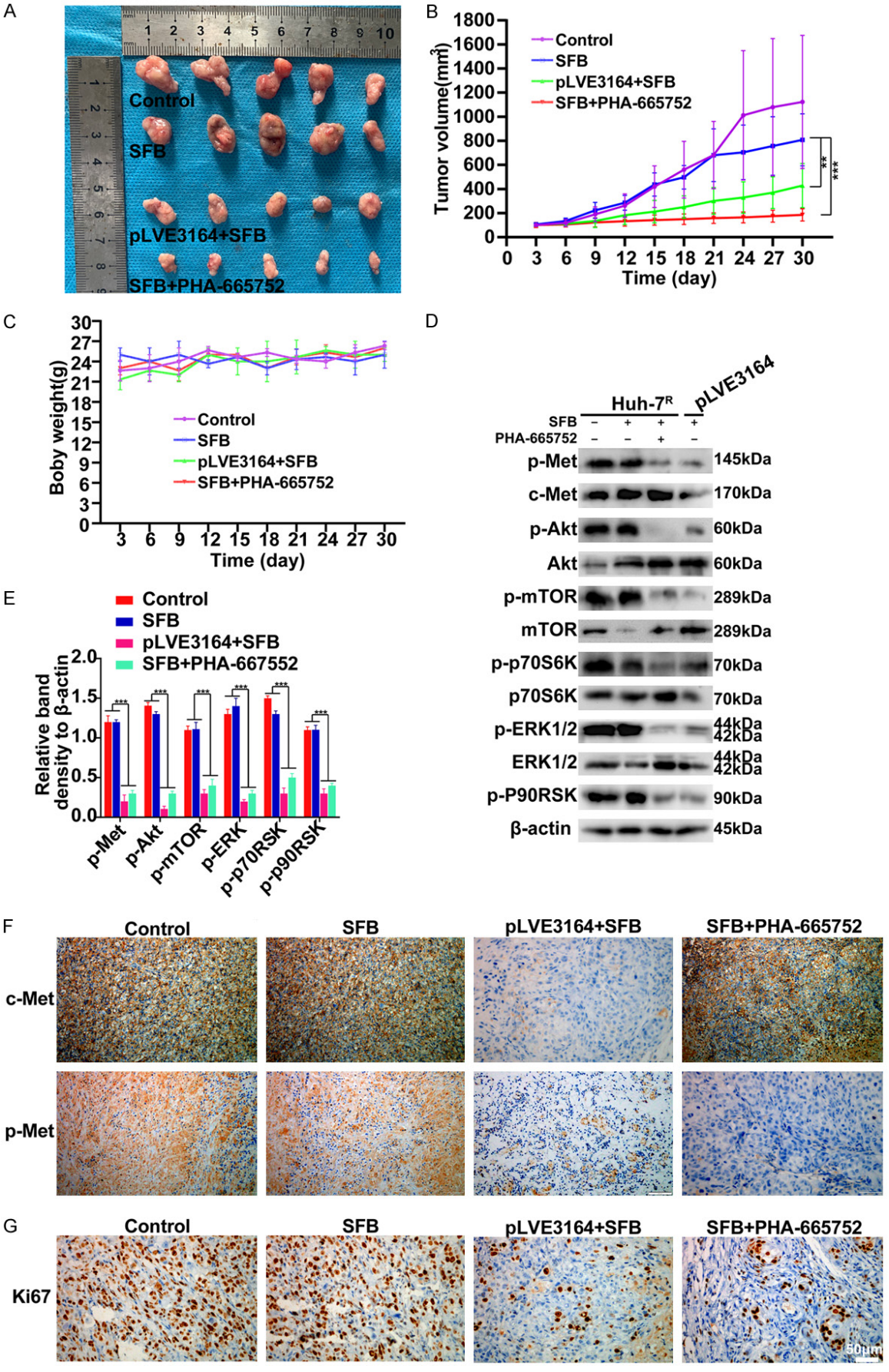
A
Control
SFB
pLVE3164+SFB
SFB+PHA-665752
B
Tumor volume(mm3)
Time (day)
Control
SFB
pLVE3164+SFB
SFB+PHA-665752
C
Boby weight(g)
Time (day)
D
Huh-7R
pLVE3164
SFB
PHA-665752
p-Met
c-Met
p-Akt
Akt
p-mTOR
mTOR
p-p70S6K
p70S6K
p-ERK1/2
ERK1/2
p-P90RSK
β-actin
145kDa
170kDa
60kDa
289kDa
70kDa
44kDa
42kDa
90kDa
45kDa
E
Relative band density to β-actin
p-Met
p-Akt
p-mTOR
p-ERK
p-p70RSK
p-p90RSK
F
Control
SFB
pLVE3164+SFB
SFB+PHA-665752
c-Met
p-Met
G
Ki67

Figure 8. Enhanced antitumor activity of sorafenib by inhibition of the expression and activation of c-Met in vivo. A. Macroscopic appearance of Huh-7^{R} and Huh-7$^{R\text{-}pLVE3164}$ xenografts of each group. B. The tumor growth curves of four groups of nude mice were recorded after 30 days of various treatments. The volume of tumors (mm^3) was recorded. C. Average body weight of mice during treatment is shown. D and E. Whole protein cell lysates from each group of tumors were prepared for western blotting to analyze the expression activation levels of relevant signaling pathways. F. Immunohistochemistry was used to detect the differences in the expression levels of c-Met and p-Met in each treatment group. G. Ki67 was used to indicate the level of proliferation in tumor tissues in each group. Images were photographed at 400× magnification. *P<0.05, **P<0.01 and ***P<0.001.

of the c-Met gene promoter. We also investigated, by western blotting and RT-PCR, whether the activation of ETS-1 was associated with the overexpression of c-Met. First, the mRNA level of c-Met was closely correlated with its protein level, which implied that the expression of this gene is transcriptionally regulated. Second, c-Met mRNA levels were highly correlated with the levels of ETS-1 protein in cells, suggesting that the transcription factor ETS-1 regulates the transcriptional expression of c-Met in HCC-resistant cell lines. Notably, we also demonstrated that the MEK/ERK signaling pathway activated the expression and activity of ETS-1 mediated by ERK, which led to its binding to the c-Met gene promoter and upregulation of c-Met transcriptional expression.

Although overexpression allows c-Met activation independent of HGF stimulation, in most cases, ligand-mediated activation is required for effective receptor activation. This is also the case for c-Met mutants that contain kinase activity that requires HGF for its activation. In this study, HGF was added in in vitro experiments to mediate the kinase activity of c-Met in Huh-7^{R} cells for studies on related mechanisms. c-Met dimerization and activation induced by HGF can regulate the cytoplasmic transduction cascade reaction through bridging molecules, thus activating multiple downstream signaling pathways, including Ras/Raf/MEK/ERK, PI3K/Akt, Jak/STAT3, and nuclear factor kappa-B (NF-κB) transduction cascades. Through these actions, biological effects such as cell proliferation, survival, migration, invasion, and epithelial mesenchymal transition result. In turn, through these associated pathways, cellular drug resistance is induced [22]. The results of this study showed that sorafenib-resistant Huh-7^{R} cells with high expression of the tyrosine kinase receptor c-Met had a resistance index RI=4.89 relative to parental Huh-7 cells (**Figure 1**), and inhibition of c-Met activation (phosphorylation) or knockdown of c-Met expression by siRNA application in Huh-7^{R} cells restored their sensitivity to sorafenib (**Figure 7**). Complete inhibition of c-Met phosphorylation (kinase activity) or silencing c-Met by siRNA inhibited the activation of the Ras/Raf/MEK/ERK and PI3K/Akt pathways (**Figures 7** and **8**). These results suggest that c-Met overexpression and aberrant activation contribute to the development of resistance to sorafenib in HCC. The resistance of HCC cells to sorafenib may be mediated through the cytoplasmic transduction cascade Ras/Raf/MEK/ERK, PI3K/Akt pathway.

Sorafenib achieves its anti-hepatoma activity mainly by targeting the vascular endothelial growth factor receptor and platelet-derived growth factor receptor to inhibit angiogenesis rather than by targeting the Raf/Mek/Erk pathway to induce apoptosis [23]. However, HCC may mediate cell proliferation and invasion and stop apoptosis in an angiogenesis-independent manner to induce acquired resistance to sorafenib through PI3K/AKT, JAK/STAT, and epithelial-mesenchymal transition pathways. Indeed, prolonged exposure of HCC cells to sorafenib activates the PI3K/AKT and JAK/STAT pathways and/or activates their downstream factors, thus contributing to sorafenib resistance [24].

The binding of the growth factors HGF and EGF to their corresponding receptors has promoted tumor cell proliferation and migration through activation of PI3K/Akt in a variety of solid tumors [12, 13, 23]. Indeed, ligand-bound tyrosine kinase receptors, such as c-Met, activate the PI3K/Akt signaling cascade, promoting cell survival, and participation in apoptosis resistance [23]. In our study, phosphorylation of Akt at serine 473 was inhibited by PHA-665752 to reverse this process. Concomitantly, the reduction of downstream Akt and ERK signaling inhibited cell migration and proliferation (**Figure 7**), which is consistent with the results of previous studies [25], and interference with c-Met expression or knockdown of c-Met inhibited the

growth of drug-resistant HCC cells with high levels of c-Met expression (**Figure 7**). c-Met-based siRNA inhibited Huh-7^R cells with tumorigenic signaling pathway activation and inhibited tumor growth. The c-Met inhibitor PHA66-5752 co-administered with sorafenib also inhibited the growth of Huh-7^R xenograft tumors (**Figure 8**), which is consistent with the results of previous studies [26].

In HCC treatment, HIF-2α triggered by sustained action activates the TGF-α/EGFR pathway [27], which in turn induces sustained activation of the downstream Ras/Raf/MAPK pathway. Also, M2-type macrophages in the HCC microenvironment activate the ERK1/2/MAPK pathway in tumor cells by secreting HGF [28]. Phosphorylated MAPK induces sorafenib resistance by phosphorylating transcription factors and regulating the expression of proteins involved in cell proliferation and resistance to apoptosis [29]. Our results showed that the phosphorylation levels of key kinases in the HGF/c-Met, PI3K/Akt, and MEK/ERK pathways were higher in Huh-7^R cells than in parental Huh-7^R cells, a result that suggests that HCC resistance to sorafenib is associated with abnormalities in the HGF/c-Met, PI3K/Akt, and MEK/ERK pathways. Further, downregulation of c-Met expression by siRNA or inhibition of c-Met phosphorylation restored the inhibition of HCC^R cell proliferation by sorafenib (**Figure 6**) and upregulated apoptosis of HCC^R cells. These results indicate that c-Met and its associated downstream MEK/ERK, and PI3K/Akt pathways are involved in the desensitization of HCC to sorafenib.

In summary, our findings in vivo and in vitro document that c-Met overexpression and overactivation regulate HCC resistance to sorafenib in HCC cells. HGF-mediated activation of c-Met rescues cells from sorafenib-induced inhibition and reactivates downstream pathways. Combining sorafenib with a c-Met inhibitor reversed HCC resistance to sorafenib by blocking HGF/c-Met signaling, downregulating important oncogenic signaling cascades, such as PI3K/Akt and MEK/ERK, and regulating related survival processes of proliferation, apoptosis, differentiation, and angiogenesis. Combining sorafenib and anti-c-Met therapy may be a strategy to circumvent sorafenib resistance in HCC.

Conclusion

HGF/c-Met induces sorafenib resistance in HCC cells by promoting cell migration, and proliferation, and stopping apoptosis, which are associated with activation of the PI3K/Akt, MAPK pathway. c-Met may be a therapeutic target for dismantling drug resistance in sorafenib-resistant HCC.

Acknowledgements

This work was supported by grants from the National Natural Science Fund of China (NO. 82071862, 81872017), University Natural Science Research Project of Anhui Province (NO. 2021sx032, 2021xjjy59), Anhui Provincial Science and Technology program (NO. 202004j07020053), University Natural Science Research Project of Anhui Province (NO. KJ2018ZD011, KJ2019A0093, KJ2020A0340) and Research Foundation of the Institute of Environment-friendly Materials and Occupational Health (Wuhu), Anhui University of Science and Technology (ALW2020YF11).

This study was approved by the Institute Review Board of First Affiliated Hospital of Anhui University of Sciences and Technology with written informed consent obtained from all patients. The animal study was approved by the Committee on the Ethics of Animal Experiments of Anhui University of Science and Technology.

Disclosure of conflict of interest

None.

Abbreviations

HCC, hepatocellular carcinoma; HGF, hepatocyte growth factor; Akt, protein kinase B; PI3K, phosphatidylinositol 3-kinase; STAT3, signal transducer and activator of transcription 3; EMT, epithelial-mesenchymal transition; SFB, sorafenib; MEK, mitogen-activated protein kinase; ERK, extracellular signal-regulated kinase; CCK-8, cell counting kit-8.

Address correspondence to: Dr. Xiaolong Tang, Medical School, Anhui University of Science and Technology, 168 Taifeng Street, Huainan 232001, Anhui, China. Tel: +86-18098691978; E-mail: txljd2006@126.com

References

[1] International Agency for Research on Cancer. GLOBOCAN 2018. IARC Available from: https://gco.iarc.fr/today/online-analysis-map?v=2020&mode=population&mode_population=continents&population=900&populations=900&key=asr&sex=0&cancer=11&type=0&statistic=5&prevalence=0&population_groupearth&color_palette=default&map_scale=quantile&map_nb_colors=5&continent=0&rotate=%255B10%252C0%255D (2020). Accessed August 19, 2021.

[2] Llovet JM, Kelley RK, Augusto V, Singal AG, Eli P, Sasan R, Riccardo L, Kazuhiko K, Zucman-Rossi J and Finn RS. Hepatocellular carcinoma (Primer). Nat Rev Dis Primers 2021; 7: 6.

[3] Global Burden of Disease Liver Cancer Collaboration, Akinyemiju T, Abera S, Ahmed M, Alam N, Alemayohu MA, Allen C, Al-Raddadi R, Alvis-Guzman N, Amoako Y, Artaman A, Ayele TA, Barac A, Bensenor I, Berhane A, Bhutta Z, Castillo-Rivas J, Chitheer A, Choi JY, Cowie B, Dandona L, Dandona R, Dey S, Dicker D, Phuc H, Ekwueme DU, Zaki MS, Fischer F, Fürst T, Hancock J, Hay SI, Hotez P, Jee SH, Kasaeian A, Khader Y, Khang YH, Kumar A, Kutz M, Larson H, Lopez A, Lunevicius R, Malekzadeh R, McAlinden C, Meier T, Mendoza W, Mokdad A, Moradi-Lakeh M, Nagel G, Nguyen Q, Nguyen G, Ogbo F, Patton G, Pereira DM, Pourmalek F, Qorbani M, Radfar A, Roshandel G, Salomon JA, Sanabria J, Sartorius B, Satpathy M, Sawhney M, Sepanlou S, Shackelford K, Shore H, Sun J, Mengistu DT, Topór-Mądry R, Tran B, Ukwaja KN, Vlassov V, Vollset SE, Vos T, Wakayo T, Weiderpass E, Werdecker A, Yonemoto N, Younis M, Yu C, Zaidi Z, Zhu L, Murray CJL, Naghavi M and Fitzmaurice C. The burden of primary liver cancer and underlying etiologies from 1990 to 2015 at the global, regional, and national level: results from the Global Burden of Disease Study 2015. JAMA Oncol 2017; 3: 1683-1691.

[4] Barsouk A, Thandra KC, Saginala K, Rawla P and Barsouk A. Chemical risk factors of primary liver cancer: an update. Hepat Med 2020; 12: 179-188.

[5] Ma Y, Xu R, Liu X, Zhang Y, Song L, Cai S, Zhou S, Xie Y, Li A, Cao W and Tang X. LY3214996 relieves acquired resistance to sorafenib in hepatocellular carcinoma cells. Int J Med Sci 2021; 18: 1456-1464.

[6] Shen J, Cai W, Ma Y, Xu R, Huo Z, Song L, Qiu X, Zhang Y, Li A, Cao W, Zhou S and Tang X. hGC33-modified and sorafenib-loaded nanoparticles have a synergistic anti-hepatoma effect by inhibiting Wnt signaling pathway. Nanoscale Res Lett 2020; 15: 220.

[7] Liu Z, Lin Y, Zhang J, Zhang Y, Li Y, Liu Z, Li Q, Luo M, Liang R and Ye J. Molecular targeted and immune checkpoint therapy for advanced hepatocellular carcinoma. J Exp Clin Cancer Res 2019; 38: 447.

[8] Leung CON, Tong M, Chung KPS, Zhou L, Che N, Tang KH, Ding J, Lau EYT, Ng IOL, Ma S and Lee TKW. Overriding adaptive resistance to sorafenib through combination therapy with Src homology 2 domain-containing phosphatase 2 blockade in hepatocellular carcinoma. Hepatology 2020; 72: 155-168.

[9] Llovet JM, Ricci S, Mazzaferro V, Hilgard P, Gane E, Blanc JF, de Oliveira AC, Santoro A, Raoul JL, Forner A, Schwartz M, Porta C, Zeuzem S, Bolondi L, Greten TF, Galle PR, Seitz JF, Borbath I, Häussinger D, Giannaris T, Shan M, Moscovici M, Voliotis D and Bruix J. Sorafenib in advanced hepatocellular carcinoma. N Engl J Med 2008; 359: 378-390.

[10] Cheng AL, Kang YK, Chen Z, Tsao CJ, Qin S, Kim JS, Luo R, Feng J, Ye S, Yang TS, Xu J, Sun Y, Liang H, Liu J, Wang J, Tak WY, Pan H, Burock K, Zou J, Voliotis D and Guan Z. Efficacy and safety of sorafenib in patients in the Asia-Pacific region with advanced hepatocellular carcinoma: a phase III randomised, double-blind, placebo-controlled trial. Lancet Oncol 2009; 10: 25-34.

[11] Tang X, Chen L, Li A, Cai S, Zhang Y, Liu X, Jiang Z, Liu X, Liang Y and Ma D. Anti-GPC3 antibody-modified sorafenib-loaded nanoparticles significantly inhibited HepG2 hepatocellular carcinoma. Drug Deliv 2018; 25: 1484-1494.

[12] Jeffers M, Rong S and Vande Woude GF. Hepatocyte growth factor/scatter factor-Met signaling in tumorigenicity and invasion/metastasis. J Mol Med (Berl) 1996; 74: 505-513.

[13] Bouattour M, Raymond E, Qin S, Cheng AL, Stammberger U, Locatelli G and Faivre S. Recent developments of c-Met as a therapeutic target in hepatocellular carcinoma. Hepatology 2018; 67: 1132-1149.

[14] Abrams ZB, Zucker M, Wang M, Asiaee Taheri A, Abruzzo LV and Coombes KR. Thirty biologically interpretable clusters of transcription factors distinguish cancer type. BMC Genomics 2018; 19: 738.

[15] Endo K, Shirai A, Furukawa M and Yoshizaki T. Prognostic value of cell motility activation factors in patients with tongue squamous cell carcinoma. Hum Pathol 2006; 37: 1111-1116.

[16] Eder JP, Vande Woude GF, Boerner SA and LoRusso PM. Novel therapeutic inhibitors of the c-Met signaling pathway in cancer. Clin Cancer Res 2009; 15: 2207-2214.

[17] Kim ES and Salgia R. MET pathway as a therapeutic target. J Thorac Oncol 2009; 4: 444-447.

[18] Tovar V, Cornella H, Moeini A, Vidal S, Hoshida Y, Sia D, Peix J, Cabellos L, Alsinet C, Torrecilla S, Martinez-Quetglas I, Lozano JJ, Desbois-Mouthon C, Solé M, Domingo-Domenech J, Villanueva A and Llovet JM. Tumour initiating cells and IGF/FGF signalling contribute to sorafenib resistance in hepatocellular carcinoma. Gut 2017; 66: 530-540.

[19] Chen W, Yang J, Zhang Y, Cai H, Chen X and Sun D. Regorafenib reverses HGF-induced sorafenib resistance by inhibiting epithelial-mesenchymal transition in hepatocellular carcinoma. FEBS Open Bio 2019; 9: 335-347.

[20] Ueki T, Fujimoto J, Suzuki T, Yamamoto H and Okamoto E. Expression of hepatocyte growth factor and its receptor, the c-met proto-oncogene, in hepatocellular carcinoma. Hepatology 1997; 25: 619-623.

[21] Bradner JE, Hnisz D and Young RA. Transcriptional addiction in cancer. Cell 2017; 168: 629-643.

[22] Garajová I, Giovannetti E, Biasco G and Peters GJ. c-Met as a target for personalized therapy. Transl Oncogenomics 2015; 7: 13-31.

[23] Sumorek-Wiadro J, Zając A, Langner E, Skalicka-Woźniak K, Maciejczyk A, Rzeski W and Jakubowicz-Gil J. Antiglioma potential of coumarins combined with sorafenib. Molecules 2020; 25: 5192.

[24] Cao W, Liu X, Zhang Y, Li A, Xie Y, Zhou S, Song L, Xu R, Ma Y, Cai S and Tang X. BEZ235 increases the sensitivity of hepatocellular carcinoma to sorafenib by inhibiting PI3K/AKT/mTOR and inducing autophagy. Biomed Res Int 2021; 2021: 5556306.

[25] Sridhar SS, Hedley D and Siu LL. Raf kinase as a target for anticancer therapeutics. Mol Cancer Ther 2005; 4: 677-685.

[26] Zhang SZ, Pan FY, Xu JF, Yuan J, Guo SY, Dai G, Xue B, Shen WG, Wen CJ, Zhao DH and Li CJ. Knockdown of c-Met by adenovirus-delivered small interfering RNA inhibits hepatocellular carcinoma growth in vitro and in vivo. Mol Cancer Ther 2005; 4: 1577-1584.

[27] Zhao D, Zhai B, He C, Tan G, Jiang X, Pan S, Dong X, Wei Z, Ma L, Qiao H, Jiang H and Sun X. Upregulation of HIF-2α induced by sorafenib contributes to the resistance by activating the TGF-α/EGFR pathway in hepatocellular carcinoma cells. Cell Signal 2014; 26: 1030-1039.

[28] Dong N, Shi X, Wang S, Gao Y, Kuang Z, Xie Q, Li Y, Deng H, Wu Y, Li M and Li JL. M2 macrophages mediate sorafenib resistance by secreting HGF in a feed-forward manner in hepatocellular carcinoma. Br J Cancer 2019; 121: 22-33.

[29] Abdel-Ghany R, Rabia I, El-Ahwany E, Saber S, Gamal R, Nagy F, Mahmoud O, Hamad RS and Barakat W. Blockade of PGE2, PGD2 receptors confers protection against prepatent schistosomiasis mansoni in mice. J Egypt Soc Parasitol 2015; 45: 511-520.